

Silicon Crystal Effects in Modeling of MEMS Silicon Resonators

S. Ghaffari, C.H. Ahn, E.J. Ng, S. Wang, and T.W. Kenny

Stanford University, Stanford, CA, USA, ghaffari@stanford.edu

ABSTRACT

We present modeling of the effects of silicon crystal properties on fundamental behavior of MEMS resonators. MEMS resonators are commonly built from single crystal silicon with proven long-term stability. It is experimentally shown that a change in crystal orientation can make up to 20% difference in the quality factor (Q) of resonators. Also, frequency splitting is observed in flexural disk resonators for anisotropic devices as well as polysilicon devices where it is not expected. We use modeling of crystal properties to predict and explain these experimental results. Tuning forks quality factor dependence on the $\langle 100 \rangle$, $\langle 110 \rangle$ and $\langle 111 \rangle$ directions and frequency splitting of disk resonators is examined. Incorporating appropriate silicon crystal elasticity values into finite-element modeling of these resonators we demonstrate that the frequency splitting and quality factor of those devices can be accurately predicted.

Keywords: Silicon anisotropy, Finite-element methods, MEMS resonator, Frequency split, Quality factor,

1 INTRODUCTION

Silicon has found considerable application in precision MEMS devices because it provides desirable high frequency and quality factor (Q) characteristics [1-5]. Single crystal silicon, in particular, is predominantly used both as substrate and the mechanical structure. Usually, MEMS resonators are built from crystalline silicon with proven long-term stability [6]. Manufacturers of precision time references, such as SiTime [7], have relied exclusively on crystalline silicon as a functional material. Silicon crystal orientation in a silicon wafer significantly affects microfabrication properties of the wafer [2] as well as the device structural behavior. Due to intrinsic anisotropy of silicon, the basic equations of elastic flexure of the device based on the Hookean relation of strain and stress depend on the orientation of the applied stress and different respective effective Young moduli (E). The value of E in planar direction varies between 130 to 188 GPa, which occur along the $\langle 100 \rangle$ and $\langle 111 \rangle$ directions respectively [8]. In practice, (100) and (111) planes are most commonly used in microfabrication therefore the effective elasticity depends on the device alignment in these planes. Because of this orientation dependence, successful prediction of the device fundamental behavior is subject to understanding and careful consideration of the anisotropy. Silicon anisotropy effect on prediction capability of the elastic behavior was recently discussed in the context of frequency

of MEMS tuning fork resonators [8]. The predicted frequency was shown to vary by almost 30%, upon incorporating the correct anisotropic elasticity. It is therefore expected that other performance parameters such as the Q be similarly affected. In fact, our experiments have shown that a change in crystal orientation can make up to 20% difference in the Q of resonators. In this paper, we present prediction of these measurement results using appropriate silicon anisotropic elasticity.

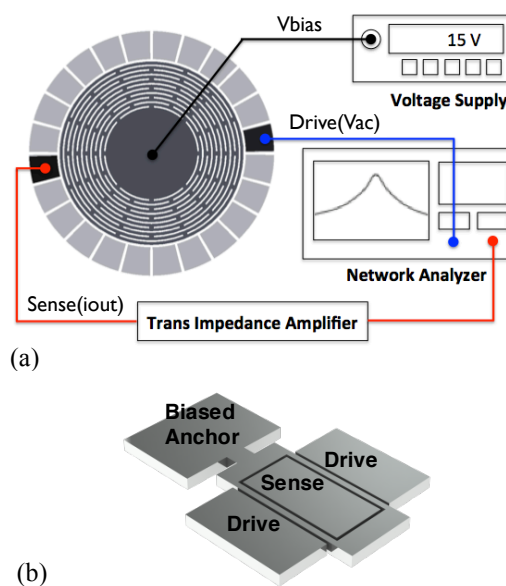


Figure 1: (a) Schematic of the disk resonator and experimental setup. (b) Schematic of a single-anchored DETF resonator with resonating beams in between sense and drive electrodes.

Many practical geometries are composed of material oriented differently in the wafer plane. When undergoing bending, the applied stress is not uniaxial and the general elasticity matrix should be used. Elasticity of silicon has orthotropic symmetry (i.e. perpendicular planes of symmetry). One interesting example is therefore flexure of axisymmetric rings. Anisotropy fixes the mode positions in the ring, which would otherwise be arbitrary and also causes a split in the natural frequencies of flexural modes. The magnitude and pattern of splitting has been shown to depend on the wafer plane in which the structure lies [9].

We have observed frequency splitting in flexural disk resonators for anisotropic devices and also isotropic polysilicon devices where it is not expected. We shall focus on prediction and explanation of these experimental results

through modeling the effects of silicon crystal properties. Incorporating silicon crystal properties into finite-element simulations of disk resonators and tuning forks, we demonstrate that the frequency splitting and quality factor of those devices can be accurately predicted.

2 METHODOLOGY

Our group has fabricated resonators in both single crystal silicon (SCS) as well as epitaxially grown polysilicon (epi-poly) [6]. SCS single-anchored, double-ended tuning forks (DETF) resonators are oriented in the $\langle 100 \rangle$, $\langle 110 \rangle$ and $\langle 111 \rangle$ directions.

We perform a set of experiments and equivalent simulations on sets of DETFs and flexural disk resonators. Each of these inherently different devices highlights the direct role of the crystal structure. Using COMSOL FEM software [10], we specifically model disk resonators for frequency splitting and tuning forks for quality factor because of our extensive experience with these devices.

To obtain the flexure modes of anisotropic structures, stress strain relationship should be implemented in terms of the anisotropic silicon stiffness matrix, C .

$$\sigma = C\varepsilon \quad (1)$$

Due to silicon cubic symmetry, only three independent elastic components remain in the fourth rank elasticity tensor. The values of these components can be obtained from the orthotropic elasticity relations as well as accurate measurements from the literature [8]. The default orthotropic stiffness matrix is formed with respect to the $\langle 100 \rangle$ cubic directions, i.e., [100], [010], and [001] and is used to calculate stress strain relationships for directions aligned with these axes. Although for the case of uniaxial stress calculations with the elasticity value along that axis are reasonably accurate, the use of the single valued E is limited to bending in the respective axis and negligible transverse bending. For multiaxial stress patterns such as the disk resonator, we resort to the orthotropic stiffness matrix as given in [8] that is solving the six simultaneous stress/strain equations (1).

Since the design alignment with respect to nominal X - Y axes on a standard (100) (or (111)) silicon wafer corresponds to different crystal orientations, i.e. [110], the default stiffness matrix must be rotated so that one of its axes aligns with the stress axis of interest. The rotated directions can be achieved in COMSOL in two ways: (1) by setting the drawing layout in the default X - Y coordinates of editor and defining the rotated orthotropic stiffness matrix for the model, (2) by rotating the drawing layout and using the default orthotropic stiffness matrix. While both approaches are equivalent, the latter has the advantage of precluding explicit matrix rotation.

For modeling the DETFs in different orientations, we use the full anisotropic elasticity matrix because of the improved prediction of measured frequency. Disk

resonators constructed from interconnected rings inherently require the matrix implementation. We obtain the natural flexure frequencies, ω , of these devices by solving the equations of motion,

$$\rho\omega^2\mathbf{u} = \nabla \cdot \sigma \quad (2)$$

The quality factor is simulated in thermoelastic limit from a fully coupled set of mechanical and thermal equations [11] where multiple thermal modes can interact significantly with the mechanical mode.

3 DISCUSSION

Vibration modes of perfect circular rings made of isotropic material should appear in degenerate pairs of equal frequency (Figure 2). Small variations in the geometry or material properties however, can cause a split in the natural frequency of the pairs [12]. For single crystal silicon (SCS), anisotropy of elastic moduli and the variation with orientation in the plane leads to frequency splitting [9]. Frequency splits of the order of 0.01% are considered practically significant.

The measured frequency response of a SCS device in the (100) plane and a polysilicon device is shown in Figure 3(a) where the peaks correspond to the disk flexure modes in Figure 2 in order of increasing frequency. The two peaks at 400 kHz belong to the mode labeled $n = 4$. Figure 3(b) shows a zoomed in view of the first peak clearly showing a split for the anisotropic device and the isotropic device. The split is largest in mode harmonics of two. However, the values of these frequency splits can increase or decrease with slight rotations of the line of applied stress with respect to the crystal principal axes.

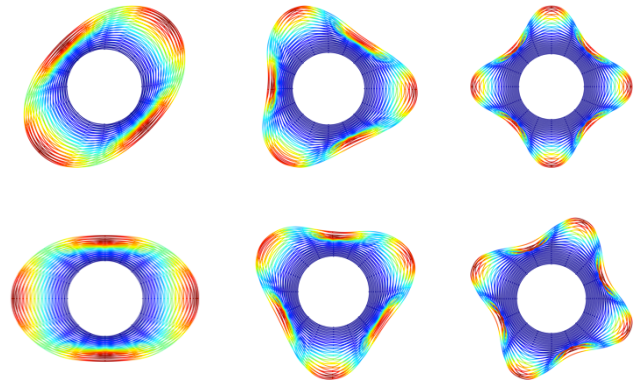


Figure 2: Simulated disk resonator flexure modes in degenerate pairs, left to right $n = 2$, $n = 3$, and $n = 4$.

Disk resonators comprising 34 circular rings connected in alternate 45° circular arcs (16 connector lines) have been modeled and experimentally tested (Figure 1(a)). Anchor pattern has 8-fold symmetry, i.e. along $\langle 100 \rangle$ and $\langle 110 \rangle$ directions. Table 1 and 2 summarize simulation and

experimental results. We first calculate the pairs of flexure mode frequencies for the anisotropic disk in its unrotated orientation, where one anchor line is along the [110] crystal direction. The simulated frequency splits from this model correspond to measurement values from three SCS devices in Table 2. By rotating the disk layout in 15° increments, we examine how the connector pattern affects the frequency split. The split values almost have a 1/16 symmetry that corresponds to one unanchored connector lines aligning with the [110] direction. However, the comparison of split values is not suggestive of a strong anchoring dependence.

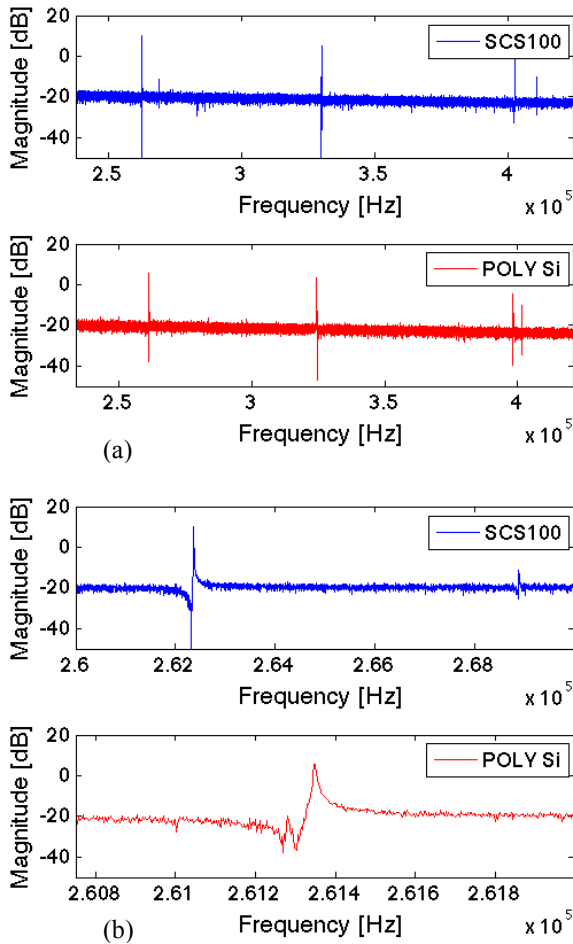


Figure 3: Measured frequency of anisotropic and isotropic disk resonator devices. (a) First four resonant modes. (b) Frequency split of the first peak.

Our models in Table 2 show comparable split values to that of measurements occur in the polysilicon disk resonator by variations as small as 0.1 μm in the width of one of the ring arcs. Such variation is reasonable from inspection of surface roughness of epi-poly device cross-section in Figure 4.

Frequency split (Hz)			
SCS (100)			
Mode no.	Device 1	Device 2	Device 3
2	5761	5765	7509
3	224	317.5	575
4	9314	9159	7994
Epi-poly			
2	84	117	174
3	228	0	39
4	3225	3326	3219

Table 1: Measured disk resonator frequency split in various devices.

Frequency split (Hz)				
SCS (100)				
Mode no.	Rotation (°)			
	0°	15°	30°	45°
2	9079	9122	9129	9090
3	4	5	0	2
4	1434	2823	2823	1435
Polysilicon				
Mode no.	No. of arcs			
	0	1	2	3
2	0	77	196	378
3	0	69	86	181
4	0	1481	2455	2442

Table 2: Simulated disk resonator frequency split with various orientations from the [110] axis for the SCS and several arcs with 0.1 μm width variation for the polysilicon.

Modeling and experiment show frequency splits of mode $n=2$ for anisotropic silicon in the (100) plane compare by less than 4%. The discrepancies for mode $n=3$ and $n=4$ may be attributed to actuation sensitivities but the simulations are consistent with the split expected from anisotropy of silicon [9]. Simulations also indicate close agreement to the theoretical limit of a silicon free ring therefore, minimized geometric dependencies (Table 3).

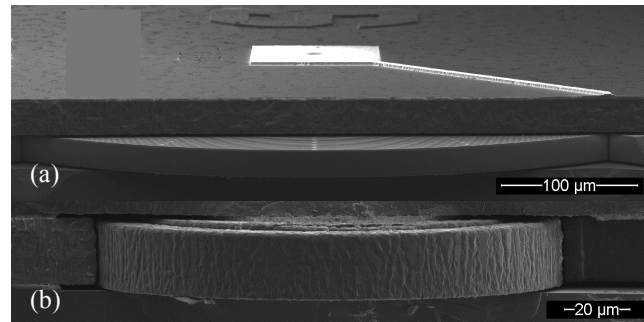


Figure 4: SEM cross-sections of the disk resonator. (a) Single crystal silicon. (b) Epi-polysilicon.

Frequency split (Hz) SCS (100)		
n = 2	n = 3	n = 4
8763	0	3200

Table 3: Simulated single frequency split of an anisotropic free ring.

Quality factor (Q) of the DETFs on the other hand, is a strong function of crystal orientation. The Q of the DETF has been previously determined to be limited by thermoelastic dissipation (TED) [11]. Figure 5 shows simulation and measurement results of temperature dependence of the Q for different orientations of the DETFs. Temperature dependencies of elastic moduli (TCE) [13] were incorporated into the simulation models. Similar behavior of polysilicon resonators to SCS resonators is noted and attributed to very similar material properties of our epi-poly to SCS. Comparison to simulation will improve by exact determination of elastic properties of epi-poly replacing the current literature values in simulations. Our simulations also indicate TED limited Q as an upper bound on total attainable Q. Because maximum and minimum stiffness occur in the $\langle 111 \rangle$ and $\langle 100 \rangle$ directions respectively, we expect the lowest and the highest Q in those directions respectively as confirmed by both measurements and simulations. Noting that the (111) plane has isotropic elastic properties [9] similarity to polysilicon results is expected.

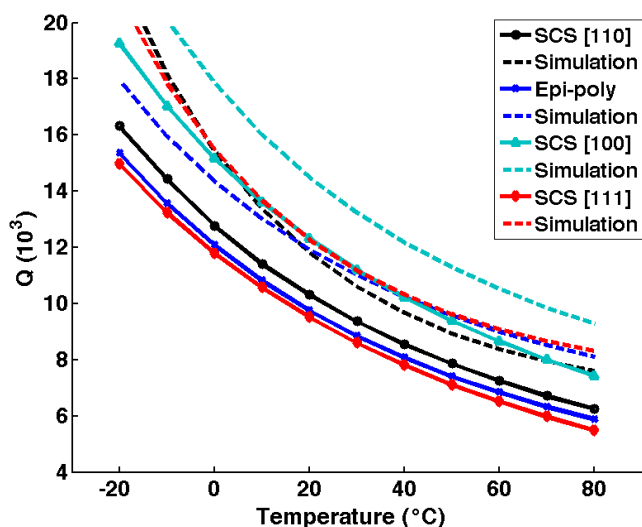


Figure 5: Temperature dependence of quality factor of single crystal silicon and epi-polysilicon double-ended tuning fork (DETF) resonators with different crystal orientations. Device schematic is shown in Figure 1(b).

4 CONCLUSION

We have modeled the effects of silicon crystal properties to predict and explain fundamental behavior of crystalline and polysilicon MEMS resonators. Frequency response of flexural disk resonators is simulated and agrees with measurement results showing frequency splitting. We also find good comparison with measurements of the temperature dependence of quality factor of tuning forks with respect to different silicon crystal orientations. Incorporating silicon crystal properties into finite-element simulations of these resonators, we have demonstrated that the frequency splitting and quality factor of those devices can be accurately predicted.

5 ACKNOWLEDGEMENTS

This work is supported by the DARPA TIMU program, managed by Dr. Andrei Shkel, through a subcontract from Honeywell Corp. Fabrication was performed at the Stanford Nanofabrication Facility. The authors would like to thank the staff at the Stanford Nanofabrication Facility.

REFERENCES

- [1] C. Liu, "Foundations of MEMS", Pearson Educ., Inc., 2006.
- [2] M. J. Madou, "Fundamentals of Microfabrication", 2nd ed., CRC Press, 2001.
- [3] S. D. Senturia, "Microsystem Design", Kluwer, 2001.
- [4] C. T.-C. Nguyen, IEEE Trans. Ultrason., Ferroelectr., Freq. Control, vol. 54, no. 2, pp. 251–270, 2007.
- [5] K. Petersen, in Proc. IEEE, vol. 70, no. 5, pp. 420–457, 1982.
- [6] R.N. Candler, W.T. Park, H.M. Li, G.Yama, A.Partridge, M. Lutz and T.W. Kenny, IEEE Trans. Adv. Packaging 26, 227, 2003.
- [7] SiTime Corporation [Online]. Available: www.sitime.com
- [8] M.A. Hopcroft, W.D. Nix, and T.W. Kenny, J. Microelectromech. Syst., vol. 19, no. 2, 2010.
- [9] R. Eley, C.H.J. Fox, S. McWilliam, J. Sound and Vibration, 228, pp. 11–35, 1999.
- [10] COMSOL Multiphysics, ver. 4.2a, 2011.
- [11] A. Duwel, R.N. Candler, T.W. Kenny, and M. Varghese, J. Microelectromech. Syst., vol. 15, no. 6, 2006.
- [12] C. H. J. Fox, J. Sound and vibration 142, pp. 227–243, 1990.
- [13] C. Bourgeois, E. Steinsland, N. Blanc, and N. F. de Rooij, in Proc. IEEE Int. Frequency Control Symp., 1997, pp. 791–799.